

Charge and current reservoirs for electric and magnetic field enhancement

Dongxing Wang,¹ Tian Yang,^{1,2} and Kenneth B. Crozier^{1,*}

¹*School of Engineering and Applied Sciences, Harvard University, Cambridge, Massachusetts 02138, USA*

²*University of Michigan-Shanghai Jiao Tong University Joint Institute, Shanghai 200240, China*

*kcrozier@seas.harvard.edu

Abstract: Two optical antenna designs incorporating structures termed charge and current reservoirs are proposed to realize localized high electric and magnetic field enhancement, respectively. Simulation results show that the fan-rod electric antenna design combines the advantages of the rod antenna and the bowtie antenna, and has higher field enhancement than either. The performance of a loop shaped magnetic antenna consisting of a pair of metallic strips with offsets is also verified numerically, with high magnetic field enhancement being observed in the simulation. In both of the designs, the concepts of charge and current reservoirs contribute to high electric and magnetic field enhancement.

©2010 Optical Society of America

OCIS codes: (240.6680) Surface plasmons; (240.6695) Surface-enhanced Raman scattering.

References and links

1. K. B. Crozier, A. Sundaramurthy, G. S. Kino, and C. F. Quate, "Optical antennas: resonators for local field enhancement," *J. Appl. Phys.* **94**(7), 4632 (2003).
2. E. Cubukcu, E. A. Kort, K. B. Crozier, and F. Capasso, "Plasmonic laser antenna," *Appl. Phys. Lett.* **89**(9), 093120 (2006).
3. N. Yu, E. Cubukcu, L. Diehl, M. A. Belkin, K. B. Crozier, F. Capasso, D. Bour, S. Corzine, and G. Höfler, "Plasmonic quantum cascade laser antenna," *Appl. Phys. Lett.* **91**(17), 173113 (2007).
4. N. Yu, E. Cubukcu, L. Diehl, D. Bour, S. Corzine, J. Zhu, G. Höfler, K. B. Crozier, and F. Capasso, "Bowtie plasmonic quantum cascade laser antenna," *Opt. Express* **15**(20), 13272–13281 (2007).
5. P. J. Schuck, D. P. Fromm, A. Sundaramurthy, G. S. Kino, and W. E. Moerner, "Improving the mismatch between light and nanoscale objects with gold bowtie nanoantennas," *Phys. Rev. Lett.* **94**(1), 017402 (2005).
6. P. Mühlischlegel, H. J. Eisler, O. J. F. Martin, B. Hecht, and D. W. Pohl, "Resonant optical antennas," *Science* **308**(5728), 1607–1609 (2005).
7. J. Aizpurua, G. W. Bryant, L. J. Richter, F. J. García de Abajo, B. Kelley, and T. Mallouk, "Optical properties of coupled metallic nanorods for field-enhanced spectroscopy," *Phys. Rev. B* **71**(23), 235420 (2005).
8. E. K. Payne, K. L. Shuford, S. Park, G. C. Schatz, and C. A. Mirkin, "Multipole plasmon resonances in gold nanorods," *J. Phys. Chem. B* **110**(5), 2150–2154 (2006).
9. E. X. Jin, and X. Xu, "Radiation transfer through nanoscale apertures," *J. Quant. Spectrosc. Radiat. Transf.* **93**(1-3), 163–173 (2005).
10. S. Nie, and S. R. Emory, "Probing single molecules and single nanoparticles by surface-enhanced Raman scattering," *Science* **275**(5303), 1102–1106 (1997).
11. J. Valentine, S. Zhang, T. Zentgraf, E. Ulin-Avila, D. A. Genov, G. Bartal, and X. Zhang, "Three-dimensional optical metamaterial with a negative refractive index," *Nature* **455**(7211), 376–379 (2008).
12. C. Yan, Y. Cui, Q. Wang, and S. Zhuo, "Negative refractive indices of a confined discrete fishnet metamaterial at visible wavelengths," *J. Opt. Soc. Am. B* **25**(11), 1815 (2008).
13. C. Yan, Y. Cui, Q. Wang, S. Zhuo, and J. Li, "Negative refraction with high transmission at visible and near-infrared wavelengths," *Appl. Phys. Lett.* **92**(24), 241108 (2008).
14. G. Shvets, and Y. A. Urzhumov, "Negative index meta-materials based on two-dimensional metallic structures," *J. Opt. A, Pure Appl. Opt.* **8**(4), S122–S130 (2006).
15. V. M. Shalaev, W. Cai, U. K. Chettiar, H.-K. Yuan, A. K. Sarychev, V. P. Drachev, and A. V. Kildishev, "Negative index of refraction in optical metamaterials," *Opt. Lett.* **30**(24), 3356–3358 (2005).
16. A. D. Rakic, A. B. Djurisic, J. M. Elazar, and M. L. Majewski, "Optical properties of metallic films for vertical-cavity optoelectronic devices," *Appl. Opt.* **37**(22), 5271–5283 (1998).
17. J. B. Pendry, A. J. Holden, D. J. Robbins, and W. J. Stewart, "Magnetism from conductors and enhanced nonlinear phenomena," *IEEE Trans. Microw. Theory Tech.* **47**(11), 2075–2084 (1999).
18. L. Ran, J. Huangfu, Y. Li, X. Zhang, K. Chen, and J. A. Kong, "Microwave solid-state left-handed material with a broad bandwidth and an ultralow loss," *Phys. Rev. B* **70**(7), 073102 (2004).

19. D. Wang, L. Ran, H. Chen, M. Mu, J. A. Kong, and B. I. Wu, "Experimental validation of negative refraction of metamaterial composed of single side paired S-ring resonators," *Appl. Phys. Lett.* **90**(25), 254103 (2007).
 20. L. Peng, L. Ran, H. Chen, H. Zhang, J. A. Kong, and T. M. Grzegorzczak, "Experimental observation of left-handed behavior in an array of standard dielectric resonators," *Phys. Rev. Lett.* **98**(15), 157403 (2007).
-

1. Introduction

Recently, the extension of antenna concepts into the optical spectral range has been explored. Through different designs of optical antennas, localized field enhancement can be conveniently realized over a range of wavelengths [1–9]. The optical antenna concept could prove useful for applications such as Surface Enhanced Raman Spectroscopy (SERS) [10] and optical metamaterials [11–15].

Traditionally, research has focused on electric optical antennas, among which, the rod antenna [2,3] and the bowtie antenna [4] have been widely investigated, because of favorable properties that include large field enhancement and subwavelength field confinement. As shown in [4], the rod antenna has a higher field enhancement factor in its center gap than the bowtie shaped antenna does, but the contrast between the enhanced fields in the center gap and the outer edge of the rod antenna is smaller than that of the bowtie antenna. In the present paper, a fan-rod antenna design with charge reservoirs is proposed to realize high field enhancement in its gap and low enhancement at its outer edge simultaneously. This work provides insight into the field enhancement mechanisms of different electric antenna structures and outlines methods to achieve high localized field enhancement. In addition to the fan-rod electric antenna design, a loop shaped optical magnetic antenna design with current reservoirs for realizing large magnetic field enhancement is also proposed in this paper. Compared with the magnetic resonant structures proposed in Refs. [13]. and [14], the loop shaped magnetic antenna with current reservoirs has higher magnetic field enhancement. The flared part of the electric antenna and the offset part of the magnetic antenna supply additional charges and currents for electric and magnetic resonances, respectively, and are therefore termed "reservoirs". The concepts of charge and current reservoirs contribute to high electric and magnetic field enhancement in both optical antenna designs.

2. Electric antenna design and magnetic antenna design

In [4], it was pointed out that the bowtie antenna has lower field enhancement than the rod antenna. The advantage of the rod antenna is its good confinement of charges at its apex, but the rod structure does not have the flared sections of the bowtie structure that work as charge reservoirs which are capable of supplying a large amount of charges. Our fan-rod electric antenna structure is shown in Fig. 1(a), and combines the advantages of both to achieve the highest enhancement among the three structures. Simulation results in the next section prove that this is the case.

The fan-rod antenna design can be divided into two parts: the rod part [gray section in Fig. 1(a)] and the flared sections (charge reservoirs). These help confine fields in the gap and reduce the accumulated charge densities at the outer edges, respectively. The fan-rod antenna design has strong electric response when it is illuminated by the incident wave with electric field polarized in the x direction and magnetic field polarized in the y direction. For comparison, the simulations of a rod antenna and a bowtie antenna [as shown in Figs. 1(b) and 1(c), respectively] are also conducted, and are described in the next section.

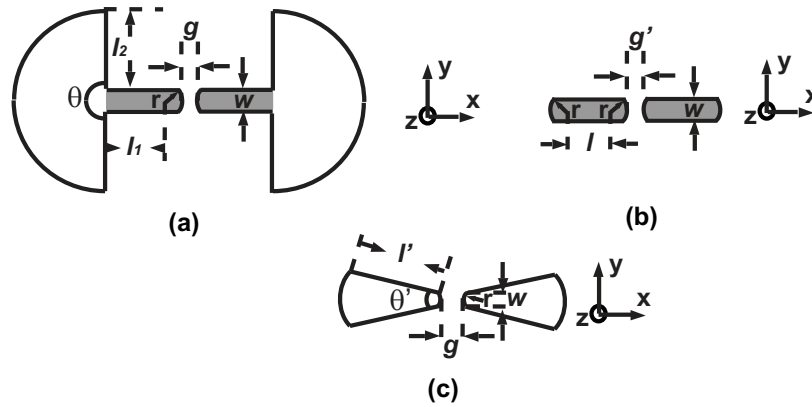


Fig. 1. (a) Fan-rod electric antenna design. (b) Rod antenna. (c) Bowtie antenna. For all of these antennas, the thickness in the z direction is 40 nm.

As a dual counterpart of the electric antenna, a small current loop with subwavelength size can be regarded as a magnetic dipole antenna. Such antennas are often used at microwave frequencies. Here, the same concept is used at optical frequencies. The unit cell of our magnetic antenna design is illustrated in Fig. 2(a).

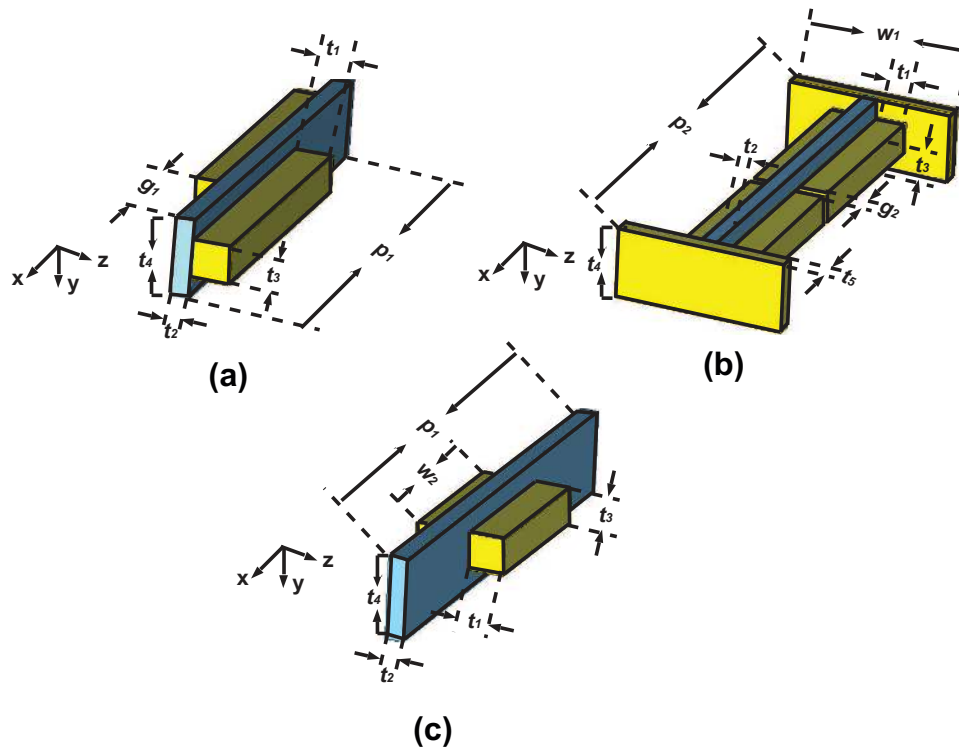


Fig. 2. (a) Unit cell of loop shaped magnetic antenna with offsets. (b) Unit cell of loop shaped magnetic antenna with slits. (c) Unit cell of loop shaped magnetic antenna without offsets. Blue parts represent free space, and are shown to aid visualization of the structures.

For the unit cell of magnetic antenna, two metallic strips [the yellow parts of Fig. 2(a)] are separated by a gap in the z direction, and offset from one another in the x direction. The metallic strips form an effective current loop enabling a magnetic resonance to be achieved. This permits the design to function as a magnetic antenna at optical frequencies. Our magnetic antenna design has strong magnetic response when it is illuminated by an incident wave with

electric field polarized in the x direction and magnetic field polarized in the y direction. The offset parts of the metallic strips work as current reservoirs that supply additional currents to the loop part of the magnetic antenna when the whole structure resonates. This property helps realize confined high magnetic field enhancement in the center of the magnetic antenna. For comparison, we also simulated the loop shaped structure with slits proposed in Ref [13], and the loop shaped structure without offsets proposed in Ref [14], in section 4. The geometries of the unit cells of the structures proposed in Ref [13], and [14] are shown in Figs. 2(b) and 2(c), respectively. In the simulations, the structures of Fig. 2 are repeated along the x direction with periodicity p_1 or p_2 and along the y direction with periodicity t_4 , respectively.

3. Performance of fan-rod electric antenna

In all simulations related to electric antennas, gold is used as the antenna material. We fit a Drude model (plasma frequency is 1.146×10^{16} rad/s and collision frequency is 1.569×10^{14} rad/s) to the optical properties of gold taken from Ref [16]. The antennas are situated in free space. The incident wave consists of a plane wave with electric field polarized in the x direction and magnetic field polarized in the y direction. The incident wave is chosen to excite the resonances of the antennas.

In experiments, electric optical antennas are often fabricated by e-beam lithography. In our experience, gaps of ~ 20 nm can be readily achieved, while gaps below 10 nm are challenging. We therefore choose an antenna gap g of 20 nm in our simulations. According to simulation results (not shown here), higher field enhancement in the center gap is achieved for rod antenna designs with thinner widths w . We believe this is due to higher charge density at the apexes. Because of the larger enhancement, the width w of the fan-rod antenna [Fig. 1(a)] is set to be 20 nm. Note that r and antenna gap are fixed, and only the lengths (l_1 , l_2 , l and l') are adjusted to make the fan-rod antenna, rod antenna and bowtie antenna all resonant at a wavelength of $\lambda = 1 \mu\text{m}$. In simulations (not shown here), we find that the field enhancement of fan-rod antenna increases when θ increases and other parameters are fixed. This is expected because larger θ indicates larger flared sections, resulting in more charges being supplied to the rod part, thereby increasing the field enhancement. We therefore choose $\theta = \pi$ to maximize the field enhancement. On the other hand, the field enhancement of the bowtie antenna decreases when θ' increases and other parameters are fixed. This is also expected because larger θ' indicates larger antenna area and higher loss as pointed out in Ref [4]. We therefore simulate bowtie antennas with $\theta' = \pi/6$, thereby achieving high field enhancement while retaining the bowtie shape.

The electric field intensity at the gap center is given in Fig. 3(a), for the fan-rod antenna ($r = 30$ nm, $l_1 = 25$ nm, $l_2 = 80$ nm, $\theta = \pi$, $w = 20$ nm and $g = 20$ nm), rod antenna ($r = 30$ nm, $l = 88$ nm, $w = 20$ nm and $g' = 20$ nm), and bowtie antenna ($r = 30$ nm, $l' = 183$ nm, $\theta' = \pi/6$, $w = 20$ nm and $g = 20$ nm). In this paper, we define the "center" of the antenna to be situated at the midpoint of the antenna gap, and 20 nm above the bottom of the antenna in the $-z$ direction. The intensity plotted is normalized to the electric field intensity of the incident wave. The geometric parameters of the three different types of antennas are chosen so that all of them are resonant at a wavelength of $\lambda = 1 \mu\text{m}$.

As shown in Fig. 3, the bowtie antenna has smaller field enhancement than the rod antenna, which is in agreement with Ref [4]. The fan-rod design has the largest field enhancement. This arises because it combines rod sections, which can confine the accumulation of charges to their apexes, with flared sections (charge reservoirs), which can supply additional charges to the apexes of the rod sections. The flared sections of fan-rod antenna are similar to the bulk metal part of the H-shaped aperture of Ref [9]. The bulk metal part of H-shaped aperture can also supply additional charges to the strip parts of the aperture, thereby achieving field enhancement. In Fig. 3(b), the field intensities along the axes of three types of antennas are shown. In this paper, we define the antenna axis as being the x axis, with the center of the antenna gap being the origin (Fig. 1). The axes of the antennas are 20 nm above the bottom of the antennas in the $-z$ direction. It can be seen that field enhancement at the outer edges of the fan-rod design is much smaller than that of the rod antenna, which is

reasonable because the flared sections reduce the charge densities at the outer edges, which naturally leads to smaller field intensity. In Fig. 3(c), the intensity distribution is shown on a plane 2 nm above the top surface of the fan-rod antenna. We find that the electric field is strongly enhanced over the antenna gap and the ratio of field intensity in the center to that at the outer edges is high. The simulation results of Fig. 3 verify that the fan-rod antenna design can simultaneously realize large field enhancement and high ratio of field intensity in the center to that at the outer edges. The large field enhancement induced by the charge reservoirs (the flared sections) suggests that fan-rod antennas could be useful for SERS.

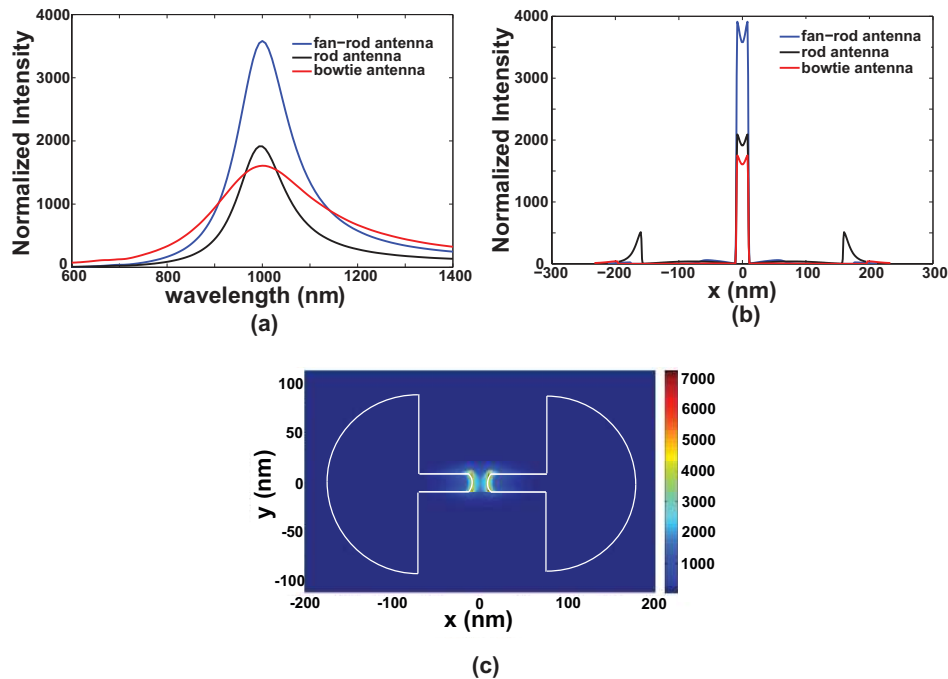


Fig. 3. (a) Normalized electric field intensity (E^2) for fan-rod antenna, rod antenna and bowtie antenna. (b) Normalized electric field intensity (E^2) profiles along antenna axes for fan-rod, rod and bowtie antennas at a wavelength of $\lambda = 1 \mu\text{m}$. (c) Normalized electric field intensity (E^2) distribution on a plane 2 nm above the top surface of the fan-rod antenna. White curves show the fan-rod antenna outline.

4. Performance of Loop-shaped Magnetic Antenna

As shown in Ref [17], [18], and [19], magnetic resonators such as split ring resonators (SRR), double side omega-shaped resonators and coplanar S-shaped resonators can be realized in the microwave frequency band where metals such as gold or copper can be regarded as perfect electric conductors (PEC). They therefore can provide surface currents to form resonant current loops. Such magnetic resonators usually have highly dispersive magnetic properties which make them useful for realizing metamaterials. In Ref [20], the authors used high permittivity nonconductive BST material to build magnetic resonators based on displacement currents at microwave frequencies. Our magnetic antenna design combines both conduction and displacement currents to form a resonant current loop. The conduction currents along the metallic strips and the displacement currents between the gaps form a current loop, as shown in Fig. 4(a). The gaps between the metallic strips introduce capacitance and the current loop introduces inductance. The unit cell of magnetic antenna can therefore be modeled by the equivalent circuit shown in Fig. 4(b). Such a design makes it feasible to tune the magnetic resonance by changing the size of the current loop and the distance between metallic strips.

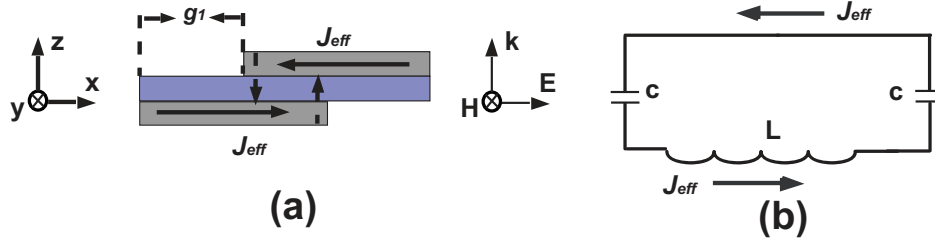


Fig. 4. (a) Current loop for the unit cell of loop shaped antenna with offsets. (b) Equivalent circuit.

For the simulations related to magnetic antennas, gold is chosen as the antenna material with the same optical properties as those of Section 3. The antennas are situated in free space. The unit cells of magnetic antennas are repeated along the x and y directions. This is realized in the simulations using periodic boundaries at the x and y direction boundaries. The incident wave is a plane wave with its electric field polarized in the x direction and its magnetic field polarized in the y direction. The incident wave is chosen to induce current in the loops of the magnetic antennas.

In simulations (not shown here), we find that magnetic field enhancement increases as t_2 decreases. We believe this is due to the magnetic field generated by conduction currents and displacement currents being stronger closer to the metallic strips. For high magnetic field enhancement, therefore, t_2 is chosen to be 20 nm for all magnetic antennas considered. To enable comparison between designs, the y direction periodicity is chosen to be the same for all magnetic antennas. In order to make all the antennas resonant at the same wavelength, we adjust the value of g_1 , p_2 and w_2 for loop shaped antenna with offsets, loop shaped antenna with slits and loop shaped antenna without offsets, respectively. As shown in Fig. 4, both the size of the current loop and the inductance in the equivalent circuit decrease when g_1 increases. By changing g_1 , the magnetic resonance of loop shaped antenna with offsets is tuned. As shown in Ref [13], and [14], the structures of Figs. 2(b) and 2(c) form current loops. Similar to loop shaped antenna with offsets, the equivalent inductance of loop shaped antenna with slits and loop shaped antenna without offsets increase when p_2 and w_2 increases. Therefore, the magnetic resonances of the loop shaped antenna with slits and the loop shaped antenna are tuned by changing p_2 and w_2 , respectively. The geometric parameters of the three different types of magnetic antennas are chosen so that all of them are resonant at a wavelength of $\lambda = 1 \mu\text{m}$.

The magnetic field intensities at the center point of the unit cells of magnetic antennas are given in Fig. 5(a), for the loop shaped antenna with offsets ($p_1 = 500$ nm, $g_1 = 142$ nm, $t_1 = 40$ nm, $t_2 = 20$ nm and $t_4 = 90$ nm), loop shaped antenna with slits ($p_2 = 552$ nm, $g_2 = 10$ nm, $t_1 = 40$ nm, $t_2 = 20$ nm, $t_3 = 20$ nm, $t_4 = 90$ nm and $w_1 = 220$ nm), and loop shaped antenna without offsets ($p_1 = 500$ nm, $w_2 = 175$ nm, $t_1 = 40$ nm, $t_2 = 20$ nm, and $t_4 = 90$ nm). The intensity plotted is normalized to the magnetic field intensity of the incident wave. The simulation results of Fig. 5(a) show that our loop shaped antenna with offsets has higher magnetic enhancement than the other two antennas at the resonant wavelength of $\lambda = 1 \mu\text{m}$. For our magnetic antenna design, we intentionally make the metallic strips have offsets. The function of the offsets is similar to that of the flared parts of the fan-rod antenna. The incident electric fields induce currents on the offsets and the offsets work as current reservoirs to inject additional currents into the loop part of the magnetic antenna. The additional currents increase the magnetic field enhancement within the current loops. To demonstrate that our magnetic antenna is a counterpart of the electric optical antenna, the distribution of the normalized magnetic field intensity for the unit cell of our magnetic antenna at the resonant wavelength of $\lambda = 1 \mu\text{m}$ is shown in Fig. 5(b). The magnetic field is tightly confined in a hot spot with subwavelength size. The full width at half maximum size of the hot spot of our magnetic antenna design is 20 nm in the z direction and 150 nm in the x direction, which is much smaller than the wavelength ($\lambda = 1 \mu\text{m}$).

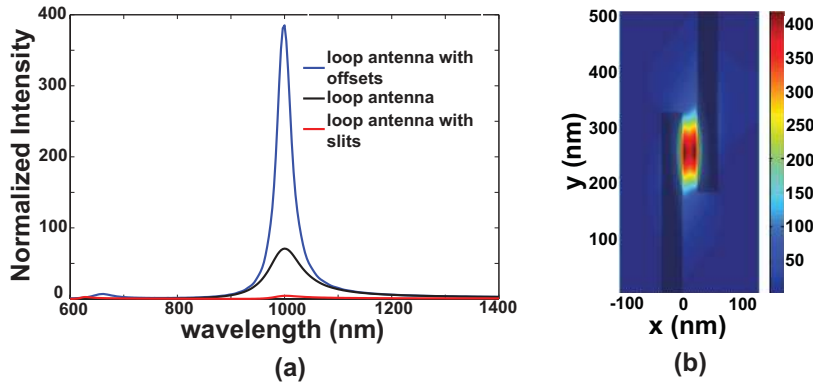


Fig. 5. (a) Normalized magnetic field intensities (H^2) for loop shaped magnetic antenna with offsets, loop shaped magnetic antenna without offsets and loop shaped magnetic antenna with slits. (b) Distribution of normalized magnetic field intensity (H^2) at a wavelength of $\lambda = 1 \mu\text{m}$ for the loop shaped magnetic antenna with offsets. The dark parts are metallic strips.

Though the hot spots of enhanced magnetic field of our magnetic antenna cannot trap nonmagnetic particles and natural magnetic particles are not available at optical frequencies, the magnetic antenna design proposed in this paper could be adjusted for trapping magnetic particles at frequencies, such as microwave frequencies, where magnetic particles are used. The high magnetic field enhancement indicates that our magnetic antenna has strong magnetic response. The performance of the metamaterials based on our magnetic antenna will be discussed in a separate paper.

6. Conclusions

We proposed two optical antennas with charge and current reservoirs: the fan-rod electric antenna and the loop shaped magnetic antenna with offsets. The charge reservoirs enable the fan-rod electric antenna to combine the advantages of the rod antenna and the bowtie antenna. A high electric field enhancement and a high ratio of field intensity in the center to that at the outer edges are simultaneously realized by our electric antenna design. By adding the current reservoirs, the loop-shaped magnetic antenna with offsets has stronger magnetic enhancement than it otherwise would. The high electric and magnetic field enhancement induced by charge and current reservoirs make our electric antenna and magnetic antenna useful for SERS, electromagnetic trapping and metamaterials. We believe the results of this paper provide insight into both electric and magnetic resonance mechanisms at optical frequencies, and will therefore enable the design of optical antennas with improved performance in the future.